Improved Microphone Array Configurations for Auralization of Sound Fields by Wave-Field Synthesis*

EDO HULSEBOS, *AES Member*, **DIEMER DE VRIES,** *AES Fellow*,
AND EMMANUELLE BOURDILLAT

Delft University of Technology, 2628 CJ Delft, The Netherlands

In order to correctly reproduce ("auralize") the acoustic wave field in a hall through a wave-field synthesis (WFS) system, impulse responses are nowadays measured along arrays of microphone positions. Three array configurations are considered–linear, cross, and circular. The linear and cross array configurations both have strong limitations, most of which can be avoided by using circular arrays. Auralization techniques are explained for all types of arrays. For the circular array configuration the connection between circular holophony, high-order incoming and outgoing ambisonics, and plane-wave decomposition for a sound field will be established and used as a tool for auralization.

0 INTRODUCTION

Perceptual evaluation and comparison between various concert halls can be done by measuring or modeling binaural impulse responses, convolving these with anechoic signals, and making them audible through headphones or near-field loudspeakers. The main shortcoming of this auralization procedure (see Naylor [1]) is that it gives only local information. Besides, sound reproduction through headphones often leads to "in-head localization," such that a good assessment of spatial cues becomes impossible.

To solve these problems a new method for auralization, based on the reproduction of multichannel impulse responses using wave-field synthesis (WFS) [2], was proposed by de Vries and Baan [3]. This method, when implemented with all its potentials, enables the perceptual assessment of the complete hall without the use of headphones, that is, including all temporal and spatial cues.

The method can be applied to both calculated impulse responses for modeled halls and measured impulse responses for existing halls. The impulse responses need to be measured on an array of microphone positions [4] in order to obtain sufficient spatial information for the correct reproduction of the physical sound field over a large listening area. Three different array configurations will be investigated—linear, cross, and circular arrays. Fig. 1 gives a sketch of the array configurations in a hall.

In order to auralize the measured impulse responses correctly, they need to be extrapolated from the recording array positions to the loudspeaker positions of the WFS system. The array recording could of course be done on microphone positions that correspond to the positions of the loudspeakers in the WFS system (holophony). No extrapolation would be required in that case. However, if one wants to do the auralization on a different WFS system with different loudspeaker positions, extrapolation is required.

Fig. 2 presents a point source and a recording array of microphones together with a WFS array of loudspeakers. The sound waves coming from the point source have to be extrapolated from the microphone array to the loudspeaker array. Since half of the microphones are in front of the loudspeaker array and half are behind the loudspeaker array, both forward and inverse wave-field extrapolation is required in this case.

To stay as general as possible, both forward and inversely extrapolated sound fields from the array configurations are considered in this paper. Loudspeaker positions of specific WFS systems can be specified afterward.

Since any sound field can be decomposed into plane waves, the plane-wave response of the array configurations will be considered first. The questions that are dealt with in this paper are: How accurate does the extrapolation

---

work from the given array configuration? How large is the area over which the recorded sound field can be correctly extrapolated/reproduced?

Kirchhoff–Helmholtz and Rayleigh integrals [5] are used for the extrapolation from linear and cross arrays. For the circular array these integrals also work but, as will be shown, it is more convenient to extrapolate the sound field using cylindrical harmonics. This will emphasize even more strongly the connection between holophony and ambisonics, as already mentioned by Nicol and Emerit [6], and present a method for recording high-order ambisonic terms using ordinary pressure and velocity microphones. (See Bamford [7] for an explanation of ambisonics.) The method used in this paper is closely related to the approach described by Poletti [8]. The main difference is that in the present paper both the incoming and the outgoing cylindrical harmonic decompositions are calculated by using both pressure and normal velocity components on the circle instead of using only the pressure. If only the pressure is used, the full cylindrical decomposition cannot be calculated, since many spatial frequency components are missing.

In this paper the circular microphone array is used for auralization purposes only, but the same theory and techniques can be applied when making live high-order ambisonic recordings.
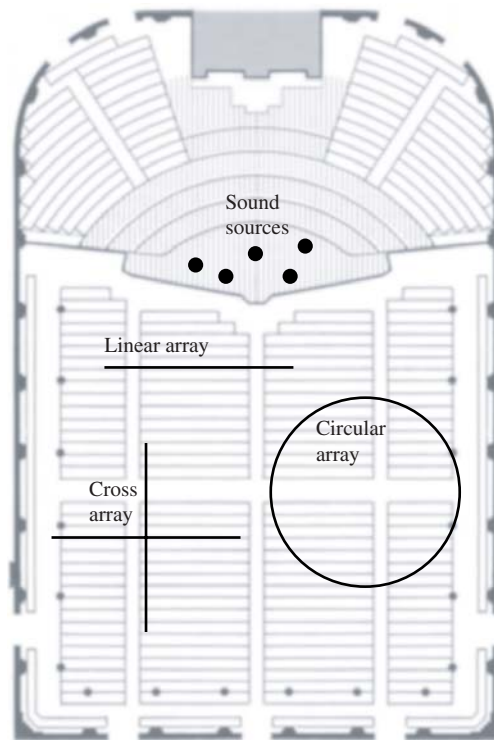
Fig. 1. Array configurations for impulse response measurements in a hall.
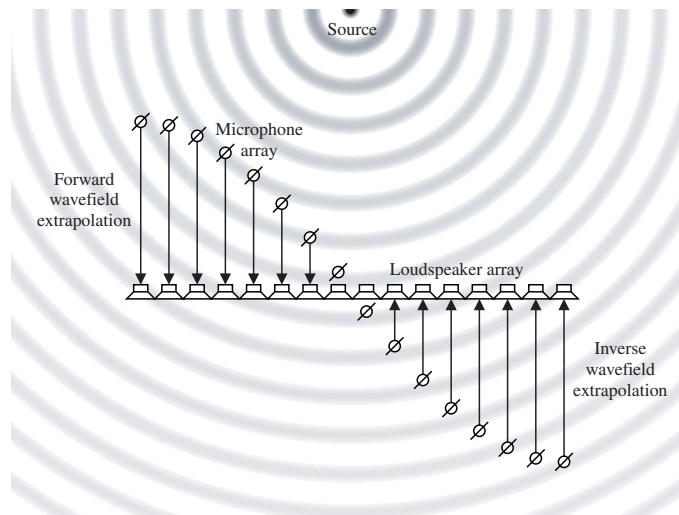
Fig. 2. Forward and inverse wave-field extrapolation from microphone array to loudspeaker array.

1 WAVE-FIELD EXTRAPOLATION

If a wave field is recorded on a linear array, it is possible to calculate the sound field at positions different from the array. According to the Huygens principle, formulated as early as 1690, each element of a wave front may be regarded as the center of an individual spherical wave. If at a later time all these individual waves are combined, the wave front at that time can be constructed. A mathematical formulation of this principle is given by the Kirchhoff–Helmholtz and Rayleigh integrals (Berkhout [5]). In this paper two-dimensional extrapolation techniques are used, since the extrapolation of sound fields from line arrays can only be done properly and consistently in two dimensions not in three. A solution for the amplitude mismatch between two- and three-dimensional sound fields will also be discussed.

1.1 Two-Dimensional Forward and Inverse Kirchhoff–Helmholtz Integrals

If both pressure and normal velocity are measured on a closed curve, the forward and inverse Kirchhoff–Helmholtz integrals can be used to extrapolate the wave field to other positions. The two-dimensional forward Kirchhoff–Helmholtz integral is given by

$$p^{(2)}(\boldsymbol{r}, \omega) = \frac{-jk}{4} \oint_C p(\boldsymbol{r}', \omega) \cos\phi \, H_1^{(2)}(k\Delta r) \, dL$$

$$+ \frac{-jk}{4} \oint_C j\rho c v_n(\boldsymbol{r}', \omega) \, H_0^{(2)}(k\Delta r) \, dL \tag{1}$$

and the two-dimensional inverse Kirchhoff–Helmholtz integral by

$$p^{(1)}(\boldsymbol{r}, \omega) = \frac{-jk}{4} \oint_C p(\boldsymbol{r}', \omega) \cos\phi \, H_1^{(1)}(k\Delta r) \, dL$$

$$+ \frac{-jk}{4} \oint_C j\rho c v_n(\boldsymbol{r}', \omega) \, H_0^{(1)}(k\Delta r) \, dL \tag{2}$$

where $H_n^{(1)}$ and $H_n^{(2)}$ are the Hankel functions of the first and second kind, respectively. Fig. 3 sketches the geometry $(\boldsymbol{r}, \boldsymbol{r}', \phi, \Delta r)$ for these integrals. $p^{(1)}$ and $p^{(2)}$ are the inverse and forward extrapolated sound fields from the array recording. The complete sound field as it can be reconstructed from the array recording is equal to the sum

$$p(\boldsymbol{r}, \omega) = p^{(1)}(\boldsymbol{r}, \omega) + p^{(2)}(\boldsymbol{r}, \omega) . \tag{3}$$

Note that the Kirchhoff–Helmholtz integrals apply to closed curves C or to curves that extend to infinity at both sides. (See Berkhout [5] for more details.)
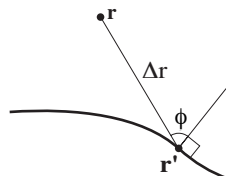
Fig. 3. Geometry for Kirchhoff–Helmholtz integral.

1.2 Two-Dimensional Forward and Inverse Rayleigh Integrals

If only the normal velocity component is measured on an infinite straight-line array, the wave field can be extrapolated using the two-dimensional forward Rayleigh I integral,

$$p^{(2)}(\boldsymbol{r}, \omega) = \frac{-jk}{2} \oint_C j\rho c v_n(\boldsymbol{r}', \omega) \, H_0^{(2)}(k\Delta r) \, dL \tag{4}$$

and the two-dimensional inverse Rayleigh I integral,

$$p^{(1)}(\boldsymbol{r}, \omega) = \frac{-jk}{2} \oint_C j\rho c v_n(\boldsymbol{r}', \omega) \, H_0^{(1)}(k\Delta r) \, dL . \tag{5}$$

If only the pressure is measured, the wave field can be extrapolated using the two-dimensional forward Rayleigh II integral,

$$p^{(2)}(\boldsymbol{r}, \omega) = \frac{-jk}{2} \oint_C p(\boldsymbol{r}', \omega) \cos\phi \, H_1^{(2)}(k\Delta r) \, dL \tag{6}$$

and the two-dimensional inverse Rayleigh II integral,

$$p^{(1)}(\boldsymbol{r}, \omega) = \frac{-jk}{2} \oint_C p(\boldsymbol{r}', \omega) \cos\phi \, H_1^{(1)}(k\Delta r) \, dL . \tag{7}$$

Note that these Rayleigh integrals only apply for infinitely long straight-line arrays. (See Berkhout [5] for more details.)

2 PLANE-WAVE DECOMPOSITION

Suppose $p^{(1)}(r, \theta, \omega)$ and $p^{(2)}(r, \theta, \omega)$ are the inverse and forward extrapolated sound fields from a given array configuration to a large circle with radius r around the origin $\boldsymbol{o}$ using the Kirchhoff–Helmholtz or Rayleigh integrals. θ is the azimuth angle on the circle (see Fig. 4). Then the plane-wave decompositions $s^{(1)}$ and $s^{(2)}$ can be calculated,

$$s^{(1)}(\theta, \omega) = \frac{1 + j}{\sqrt{4\pi}} \lim_{r \to \infty} \sqrt{kr} \, p^{(1)}(r, \theta, \omega) \, e^{-jkr}$$

$$s^{(2)}(\theta, \omega) = \frac{1 - j}{\sqrt{4\pi}} \lim_{r \to \infty} \sqrt{kr} \, p^{(2)}(r, \theta, \omega) \, e^{jkr} . \tag{8}$$

The derivation of these equations can be found in Appendix 1. These plane-wave decompositions give a complete description of the sound field, and not only in the origin, since plane waves can easily be extrapolated to any position,

$$p^{(1)}(r, \theta, \omega) = \int_0^{2\pi} s^{(1)}(\theta', \omega) \, e^{-jkr \cos(\theta - \theta')} \, d\theta'$$

$$p^{(2)}(r, \theta, \omega) = \int_0^{2\pi} s^{(2)}(\theta', \omega) \, e^{jkr \cos(\theta - \theta')} \, d\theta' . \tag{9}$$

Thus the plane-wave decomposition is a flexible format, which can be used to calculate the sound field at any position, and is therefore very suitable for auralization purposes.

3 LINEAR ARRAYS

Three types of linear arrays are considered—the linear monopole array, the linear dipole array, and the linear hypercardioid array.

3.1 Linear Monopole Array

The extrapolation for the linear monopole array, consisting of pressure microphones, can be done using the Rayleigh II integrals, Eqs. (6) and (7),

$$p^{(1)}(r,\theta,\omega) = \frac{-jk}{2} \int_L p(x,\omega) \cos \phi \, H_1^{(1)}(k\Delta r) \, dx \tag{10}$$

$$p^{(2)}(r,\theta,\omega) = \frac{-jk}{2} \int_L p(x,\omega) \cos \phi \, H_1^{(2)}(k\Delta r) \, dx .$$

Fig. 5 gives an explanation of r, θ, Δr, ϕ, and x.

Using the far-field approximation of Eqs. (31) in Appendix 1 together with

$$\cos \phi \approx \cos \theta , \quad \Delta r \approx r + x \sin \theta \tag{11}$$

results in

$$p^{(1)}(r,\theta,\omega) \approx \frac{(-1+j)k}{2} \cos \theta \, \frac{e^{jkr}}{\sqrt{\pi kr}} \int_L p(x,\omega) \, e^{jkx \sin \theta} \, dx$$

$$p^{(2)}(r,\theta,\omega) \approx \frac{(-1-j)k}{2} \cos \theta \, \frac{e^{-jkr}}{\sqrt{\pi kr}} \int_L p(x,\omega) \, e^{-jkx \sin \theta} \, dx . \tag{12}$$

From this extrapolation the plane-wave decomposition can be calculated using Eqs. (11),

$$s^{(1)}(\theta,\omega) = \frac{k}{2\pi} \cos \theta \int_L p(x,\omega) \, e^{jkx \sin \theta} \, dx$$

$$s^{(2)}(\theta,\omega) = \frac{k}{2\pi} \cos \theta \int_L p(x,\omega) \, e^{-jkx \sin \theta} \, dx . \tag{13}$$

Fig. 6(a) illustrates the reconstruction of a plane wave, incident under a 30° angle on a 4-m-long linear monopole array. As can be seen from the figure, the linear monopole array is not able to discriminate between waves incident from the front and waves incident under the corresponding angle from the back. Both wave types are reconstructed, as can be seen. Therefore the linear monopole array is not suitable for auralization purposes. Also strong artifacts from the endpoints of the array are visible. This is because
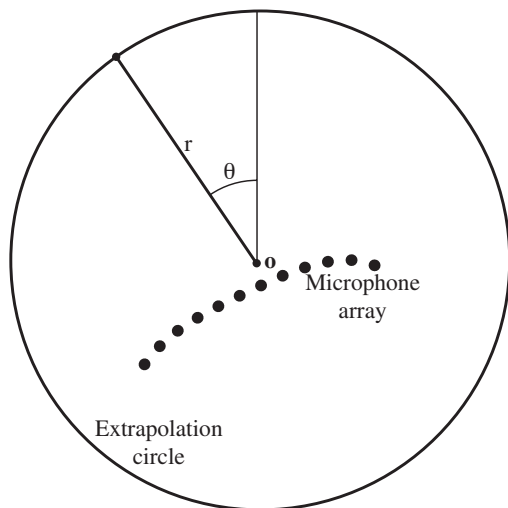
the array is finite whereas Rayleigh integral works only for infinite arrays. These artifacts can be reduced to some extent by smooth tapering of the endpoints of the array.

3.2 Linear Dipole Array

The extrapolation for the linear dipole array, which consisted of velocity microphones, can be done using the Rayleigh I integrals,

$$p^{(1)}(r,\theta,\omega) = \frac{-jk}{2} \int_L j\rho c v_n(x,\omega) \, H_0^{(1)}(k\Delta r) \, dx$$

$$p^{(2)}(r,\theta,\omega) = \frac{-jk}{2} \int_L j\rho c v_n(x,\omega) \, H_0^{(2)}(k\Delta r) \, dx . \tag{14}$$

Using the far-field approximations from Eqs. (11) and (31) and substituting in the plane-wave decomposition

from Eqs. (8) results in

$$s^{(1)}(\theta,\omega) = \frac{k}{2\pi} \int_L \rho c v_n(x,\omega) \, e^{jkx \sin \theta} \, dx$$

$$s^{(2)}(\theta,\omega) = \frac{k}{2\pi} \int_L \rho c v_n(x,\omega) \, e^{-jkx \sin \theta} \, dx . \tag{15}$$

Fig. 6(b) shows the reconstruction of a plane wave incident on a 4-m-long linear dipole array. As can be seen, the linear dipole array is also not able to discriminate between the waves incident from the front and those from the back. Once again both wave types are reconstructed. Therefore the linear dipole array too is not suitable for auralization purposes. Furthermore, artifacts from the endpoints are present.

Fig. 4. r, θ.
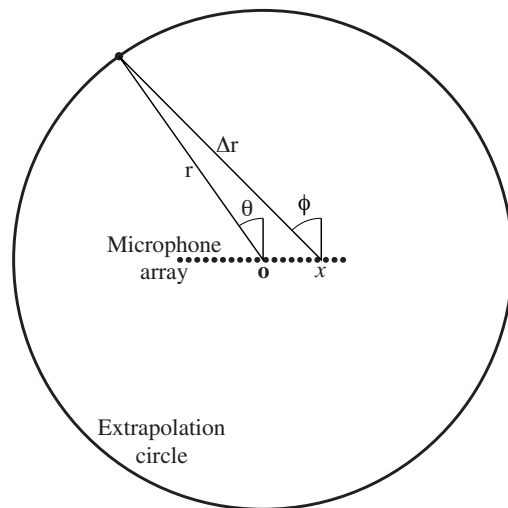
Fig. 5. r, θ, Δr, ϕ, x.

3.3 Linear Hypercardioid Array

If both pressure and normal velocity are recorded on a line array, the sound field can be extrapolated using the Kirchhoff–Helmholtz integrals,

$$p^{(1)}(r, \theta, \omega) = \frac{-jk}{2} \int_L j\rho c v_n(x, \omega) H_0^{(1)}(k\Delta r) \, dx$$

$$+ \frac{-jk}{2} \int_L p(x, \omega) \cos \phi \, H_1^{(1)}(k\Delta r) \, dL$$

$$(16)$$

$$p^{(2)}(r, \theta, \omega) = \frac{-jk}{2} \int_L j\rho c v_n(x, \omega) H_0^{(2)}(k\Delta r) \, dx$$

$$+ \frac{-jk}{2} \int_L p(x, \omega) \cos \phi \, H_1^{(2)}(k\Delta r) \, dL \, .$$

Using again the far-field approximations from Eqs. (11) and (31), the plane-wave decompositions from Eqs. (8) for the linear cardioid array become

$$s^{(1)}(\theta, \omega) = \frac{k}{2\pi} \int_L \left[\rho c v_n(x, \omega) + \cos \theta \, p(x, \omega) \right] e^{jkx \sin \theta} \, dx$$

$$s^{(2)}(\theta, \omega) = \frac{k}{2\pi} \int_L \left[\rho c v_n(x, \omega) + \cos \theta \, p(x, \omega) \right] e^{-jkx \sin \theta} \, dx.$$

$$(17)$$

Fig. 6(c) shows the reconstruction of a plane wave incident on a 4-m-long linear hypercardioid array. Unlike the previously discussed linear arrays, the combined pressure and velocity array is capable of discriminating between front and rear.

How this discrimination comes about can be seen by looking at the term $\rho c v_n + \cos \theta \, p$ in Eqs. (17). The first term $\rho c v_n$ is recorded with figure-of-eight microphone whereas for the second term p an omnidirectional microphone is used. By multiplying the omnidirectional microphone signal with $\cos \theta$ and combining it with the figure-of-eight microphone, a θ-dependent hypercardioid microphone is obtained. The directivity pattern of this hypercardioid microphone is sketched in Fig. 7 for different angles θ. Note that each hypercardioid has zero sensitivity at the angle from which the rear event is coming that needs to be eliminated. Due to finiteness the artifacts from the endpoints still exist.

3.4 Reconstruction Area

The proper reconstruction area of the linear hypercardioid array is considered next. In Fig. 6(c) it can already be seen that the reconstruction area of the 30° incident plane wave is limited by the aperture of the array. Fig. 8(a) shows the reconstruction of plane-wave events under various angles. The plane wave incident under 90° has only a very narrow strip around the array on which it is properly reconstructed. This is due to the limited angular resolution
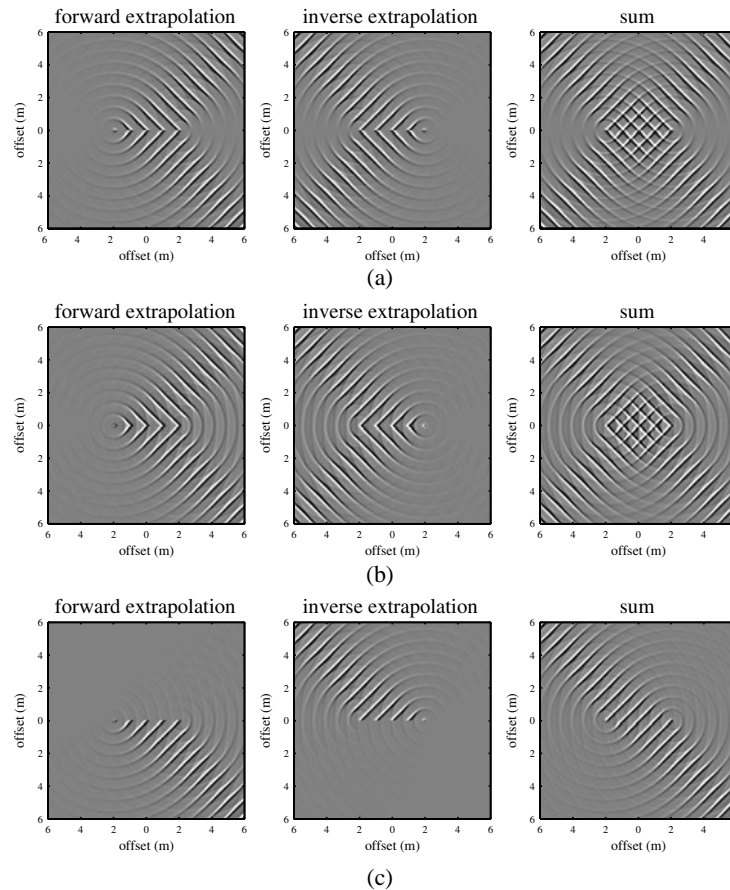
Fig. 6. Reconstruction of plane wave by forward and inverse wave-field extrapolation. (a) Using monopole array. (b) Using dipole array. (c) Using hypercardioid array.

of a linear array in endfire configuration. This very narrow reproduction strip makes the linear array unsuitable for auralization purposes.

4 CROSS ARRAY

In order to compensate for the limited reconstruction area of a linear hypercardioid array, two linear arrays can be combined in a cross array. In this manner the limited angular resolution in the endfire configuration of one array can be improved by using the other. This can be done by combining the plane-wave decompositions of the two arrays, where w and u are weighting functions, which should satisfy

$$w(\theta) + u(\theta) = 1 \qquad (19)$$

for all θ. Furthermore they should be chosen such that when θ comes closer to the endfire configuration for one array, the other array takes over smoothly. A suitable choice for these weighting functions would be

$$w(\theta) = \cos^2 \theta \quad \text{and} \quad u(\theta) = \sin^2 \theta . \qquad (20)$$

Fig. 8(b) shows the reconstructions of plane waves with different angles of incidence using a cross array with these

$$
\begin{aligned}
s^{(1)}(\theta, \omega) = \frac{k}{2\pi} \; w(\theta) \int_{L_1} \left\{ \rho c v_n(x, \omega) + \cos\theta \; p(x, \omega) \right\} e^{jkx \sin\theta} \, dx \\
+ \frac{k}{2\pi} \; u(\theta) \int_{L_2} \left\{ \rho c v_n(y, \omega) + \sin\theta \; p(y, \omega) \right\} e^{jky \cos\theta} \, dy
\end{aligned}
\qquad (18)
$$
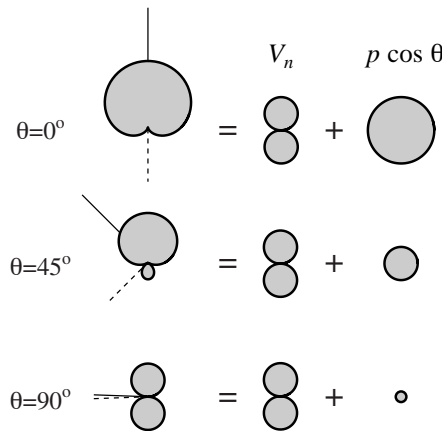
Fig. 7. θ-dependent directivity patterns of hypercardioid microphone.
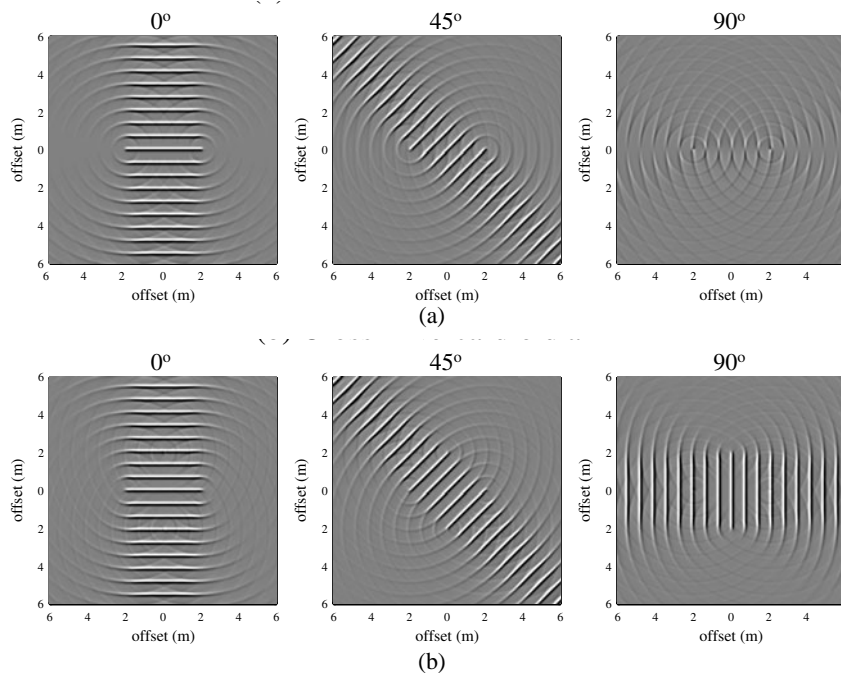
Fig. 8. Reconstruction of plane waves under various angles. (a) Using hypercardioid linear array. (b) Using hypercardioid cross array.

weighting functions. Note that the reconstruction area has become much larger, but the reconstruction still is not perfect. Diffraction effects are visible from the endpoints of the arrays, and the amplitude of the plane wave is not constant over the entire reproduction area.

5 CIRCULAR ARRAY

In this section a circular microphone array is considered. If both pressure and normal particle velocity are recorded on a circle, the complete sound field within the circle can be reconstructed using the Kirchhoff–Helmholtz integrals. Suppose the circle has a radius R. If $p(\theta, \omega)$ and $v_n(\theta, \omega)$ represent the pressure and particle velocity on the circular array, where θ is the azimuth angle, the two-dimensional Kirchhoff–Helmholtz integrals become

$$p^{(1)}(\mathbf{r}, \omega) = \frac{-jk}{4} \int_0^{2\pi} p(\theta, \omega) \cos \phi \, H_1^{(1)}(k\Delta r) R \, d\theta$$
$$+ \frac{-jk}{4} \int_0^{2\pi} j\rho c v_n(\theta, \omega) H_0^{(1)}(k\Delta r) R \, d\theta$$

(21)

$$p^{(2)}(\mathbf{r}, \omega) = \frac{-jk}{4} \int_0^{2\pi} p(\theta, \omega) \cos \phi \, H_1^{(2)}(k\Delta r) R \, d\theta$$
$$+ \frac{-jk}{4} \int_0^{2\pi} j\rho c v_n(\theta, \omega) H_0^{(2)}(k\Delta r) R \, d\theta .$$

Fig. 9 shows the reconstruction of a circular recording for p and v_n of a plane wave at $t = 0$. Notice that the Kirchhoff–Helmholtz integrals are only capable of reconstructing the sound field within the circle. Outside the circle the field becomes zero. For this reason it is impossible to calculate the plane-wave decomposition using Eqs. (8). However, in the next section the circular recording is extrapolated using cylindrical harmonics. In that case the sound field is no longer limited to the interior of the circle and the plane-wave decomposition becomes possible.

5.1 Cylindrical Harmonics

The next approach is to decompose the sound field, as it is recorded on a circular array, into cylindrical harmonics. Cylindrical harmonics are the two-dimensional variant of spherical harmonics. (See [7] and [9] for an explanation of spherical and cylindrical harmonics.) The sound field of monopole and dipole sound sources can be seen as

zero- and first-order spherical or cylindrical harmonics. In two dimensions the sound fields of these and higher order cylindrical harmonics are given by

$$\mathscr{P}_{k_\theta}^{(1)}(r, \theta, \omega) = H_{k_\theta}^{(1)}(kr) \, e^{jk_\theta \theta}$$

(22)

$$\mathscr{P}_{k_\theta}^{(2)}(r, \theta, \omega) = H_{k_\theta}^{(2)}(kr) \, e^{jk_\theta \theta}$$

which represent the pressure fields of the incoming and outgoing cylindrical harmonics, respectively. Outgoing cylindrical harmonics can be thought of as the sound field caused by multipole sources at the origin and ingoing cylindrical harmonics as the sound field caused by multipole wells. k_θ is the order of the harmonic and can be any positive or negative integer number. The sound field of a monopole corresponds to the case $k_\theta = 0$ and the dipole field can be obtained by taking an appropriate linear combination of $\mathscr{P}_{-1}^{(2)}$ and $\mathscr{P}_1^{(2)}$.

In Appendix 2 a derivation is given for the decomposition of a recorded sound field on a circular array in terms of cylindrical harmonics. This decomposition is given by

$$\mathscr{M}^{(1)}(k_\theta, \omega)$$

$$= \frac{H_{k_\theta}'^{(2)}(kR) \, P(k_\theta, \omega) - H_{k_\theta}^{(2)}(kR) \, j\rho c V_n(k_\theta, \omega)}{H_{k_\theta}^{(1)}(kR) H_{k_\theta}'^{(2)}(kR) - H_{k_\theta}^{(2)}(kR) H_{k_\theta}'^{(1)}(kR)}$$

(23)

$$\mathscr{M}^{(2)}(k_\theta, \omega)$$

$$= \frac{H_{k_\theta}'^{(1)}(kR) \, P(k_\theta, \omega) - H_{k_\theta}^{(1)}(kR) \, j\rho c V_n(k_\theta, \omega)}{H_{k_\theta}^{(2)}(kR) H_{k_\theta}'^{(1)}(kR) - H_{k_\theta}^{(1)}(kR) H_{k_\theta}'^{(2)}(kR)}$$

where $\mathscr{M}^{(1)}$ and $\mathscr{M}^{(2)}$ are the expansion coefficients of the sound field in terms of cylindrical harmonics [see Eqs. (39), Appendix 2]. Bamford [7] describes the decomposition and reproduction of sound fields in terms of spherical and cylindrical harmonics, which is called ambisonics. Therefore $\mathscr{M}^{(1)}$ and $\mathscr{M}^{(2)}$ will denote the incoming and outgoing ambisonic representations of the sound field. Notice that with the circular array it is possible to record ambisonic terms of all orders, whereas until now ambisonic recordings have been using Soundfield microphone [10], [12], which is limited to first order ($k_\theta = -1, 0, 1$).
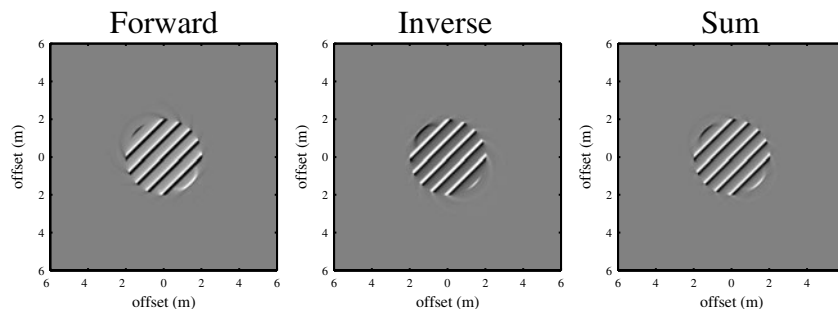
Fig. 9. Reconstruction of circular recording using Kirchhoff–Helmholtz integral.

In principle the sound field at any point in space can be reconstructed from $\mathscr{M}^{(1)}$ and $\mathscr{M}^{(2)}$ using

$$p(r,\theta,\omega) = \sum_{k_\theta} \mathscr{M}^{(1)}(k_\theta,\omega)\, \mathscr{P}^{(1)}_{k_\theta}(r,\theta,\omega)$$
$$+ \sum_{k_\theta} \mathscr{M}^{(2)}(k_\theta,\omega)\, \mathscr{P}^{(2)}_{k_\theta}(r,\theta,\omega)$$
$$\qquad (24)$$
$$v_n(r,\theta,\omega) = \sum_{k_\theta} \mathscr{M}^{(1)}(k_\theta,\omega)\, \mathscr{V}^{(1)}_{k_\theta}(r,\theta,\omega)$$
$$+ \sum_{k_\theta} \mathscr{M}^{(2)}(k_\theta,\omega)\, \mathscr{V}^{(2)}_{k_\theta}(r,\theta,\omega)\,.$$

In practice this only goes well for $r > R$, since for $r < R$ the Hankel functions in $\mathscr{P}^{(1,2)}_{k_\theta}$ and $\mathscr{V}^{(1,2)}_{k_\theta}$ become very large for large k_θ. The sum of these extremely large numbers with opposite signs for different k_θ is finite and results in the correct solution. However, the calculation is not possible using normal precision floating-point numbers. The extrapolation to larger circles than the array is no problem, however. A plane-wave decomposition of the ambisonic sound field given by Eqs. (24) is derived next, from which the reconstruction is much easier.

5.2 Plane-Wave Decomposition

For the incoming and outgoing parts of the wave field the pressure can be calculated on any circle,

$$p^{(1)}(r,\theta,\omega) = \sum_{k_\theta} \mathscr{M}^{(1)}(k_\theta,\omega)\, \mathscr{P}^{(1)}_{k_\theta}(r,\theta,\omega)$$
$$\qquad (25)$$
$$p^{(2)}(r,\theta,\omega) = \sum_{k_\theta} \mathscr{M}^{(2)}(k_\theta,\omega)\, \mathscr{P}^{(2)}_{k_\theta}(r,\theta,\omega)$$

where r is the radius and θ the azimuth angle. If we substitute these equations into the plane-wave decomposition given by Eqs. (8), the plane-wave decomposition of the sound field in terms of the cylindrical harmonics becomes

$$s^{(1)}(\theta,\omega) = \frac{1+\mathrm{j}}{\sqrt{4\pi}} \lim_{kr\to\infty} \sqrt{kr}\, \mathrm{e}^{-\mathrm{j}kr}$$
$$\times \sum_{k_\theta} \mathscr{M}^{(1)}(k_\theta,\omega)\, H^{(1)}_{k_\theta}(kr)\, \mathrm{e}^{-\mathrm{j}k_\theta\theta}$$
$$\qquad (26)$$
$$s^{(2)}(\theta,\omega) = \frac{1-\mathrm{j}}{\sqrt{4\pi}} \lim_{kr\to\infty} \sqrt{kr}\, \mathrm{e}^{\mathrm{j}kr}$$
$$\times \sum_{k_\theta} \mathscr{M}^{(2)}(k_\theta,\omega)\, H^{(2)}_{k_\theta}(kr)\, \mathrm{e}^{-\mathrm{j}k_\theta\theta}$$

If the far-field approximations of Eqs. (31) are used for the Hankel functions, this becomes

$$s^{(1)}(\theta,\omega) = \frac{1}{2\pi} \sum_{k_\theta} \mathrm{j}^{(1-k_\theta)}\, \mathscr{M}^{(1)}(k_\theta,\omega)\, \mathrm{e}^{\mathrm{j}k_\theta\theta}$$
$$\qquad (27)$$
$$s^{(2)}(\theta,\omega) = \frac{1}{2\pi} \sum_{k_\theta} \mathrm{j}^{(1+k_\theta)}\, \mathscr{M}^{(2)}(k_\theta,\omega)\, \mathrm{e}^{\mathrm{j}k_\theta\theta}\,.$$

This is a very remarkable result, which states that the plane-wave decomposition of the complex ambisonic sound field is up to a factor equal to the inverse Fourier transform of the ambisonic representation. It is important to notice that the $=$ signs in these equations are exact, since the far-field approximations made to derive the plane-wave decomposition become exact in infinity. Using Eqs. (9) the complete sound field can be reconstructed easily from the plane waves, and the instability from the Hankel functions when using Eqs. (24) for the reconstruction can be avoided. Fig. 10(a) shows the reconstruction of a plane wave, recorded using a circular array, decomposed into complex cylindrical harmonics using Eqs. (23), and converted into a plane-wave decomposition using Eqs. (27). Within the circle the reconstruction is very good. There are no artifacts.

The question may now arise how the circular array will respond to wave events other than plane waves. Therefore a number of circular recordings of point sources are used, and both incoming and outgoing wave fields are reconstructed [Fig. 10(b), (c)]. Note that all sound fields are reconstructed within the circle without any artifacts. Also note that for plane waves and point sources outside the circular array the reconstruction of the incoming part is equal to the outgoing part. However, sound waves of sources inside the circle are present only in the outgoing part and are absent in the incoming part. This way it is possible to eliminate such sources in the reproduction by reproducing only the incoming part of the sound field.

6 USING TWO-DIMENSIONAL TECHNIQUES FOR THREE-DIMENSIONAL HALLS

In this paper two-dimensional techniques are used for reconstructing sound fields. However, if the sound field recordings are done in three-dimensional rooms using line arrays of microphones, the extrapolation of such a recording is not correct.

6.1 Amplitude Errors

First of all, in three dimensions the decay of a point source is $1/r$, whereas in two dimensions the (far-field) decay is $1/\sqrt{r}$. The two-dimensional extrapolated field also had a $1/\sqrt{r}$ decay, which does not match the real decay. If arbitrary sound fields are recorded, such as live music registration through a circular array, these amplitude errors cannot be corrected. However, when impulse responses are measured, which is the case for auralization, the events in measured impulse responses that have a three-dimensional amplitude decay can be converted to two dimensions since for each of these events the travel time (which is equal to the arrival time), and thus the travel distance, is known.

Suppose $p^{(3\mathrm{D})}(x, t)$ is a measured impulse response. Then a spherical event arriving at time t will have traveled a distance $r = t$ and in three-dimensional space will have an amplitude attenuation of $1/r = 1/ct$. In two-dimensional space this event would have an amplitude gain of $1/\sqrt{r} = 1/\sqrt{ct}$. To convert the three-dimensional spherical event to a two-dimensional one, the former needs to be multiplied

by $\sqrt{r} = \sqrt{ct}$. Thus for the whole impulse response this becomes

$$p^{(2D)}(x,t) = \sqrt{ct}\ p^{(3D)}(x,t) . \tag{28}$$

After the extrapolation process the two-dimensional sound field can be converted back to three dimensions by

$$p^{(3D)}(x,t) = \frac{p^{(2D)}(x,t)}{\sqrt{ct}} . \tag{29}$$

The singularity of $1/\sqrt{ct}$ at $t = 0$ poses no real problem since all sound events in an impulse response arrive at a later time than $t = 0$. Note that this amplitude scaling for recordings in a hall only works properly for spherical events (direct sound, mirror reflections) and thus may not be correct for other events (diffractions).

6.2 Elevation Angles

A second inaccuracy encountered when using line array configurations in three-dimensional space is the reconstruction of elevated sound sources. For example, a sound source coming from right above the center of a circular array will give the same response at the array as the combination of two sources, one outgoing sound source and one incoming sound well at the center of the circle. The reconstruction will therefore be incorrect. Thus if a line array is used for auralization purposes of a hall, one needs to be aware of the fact that ceiling reflections are not properly reproduced.
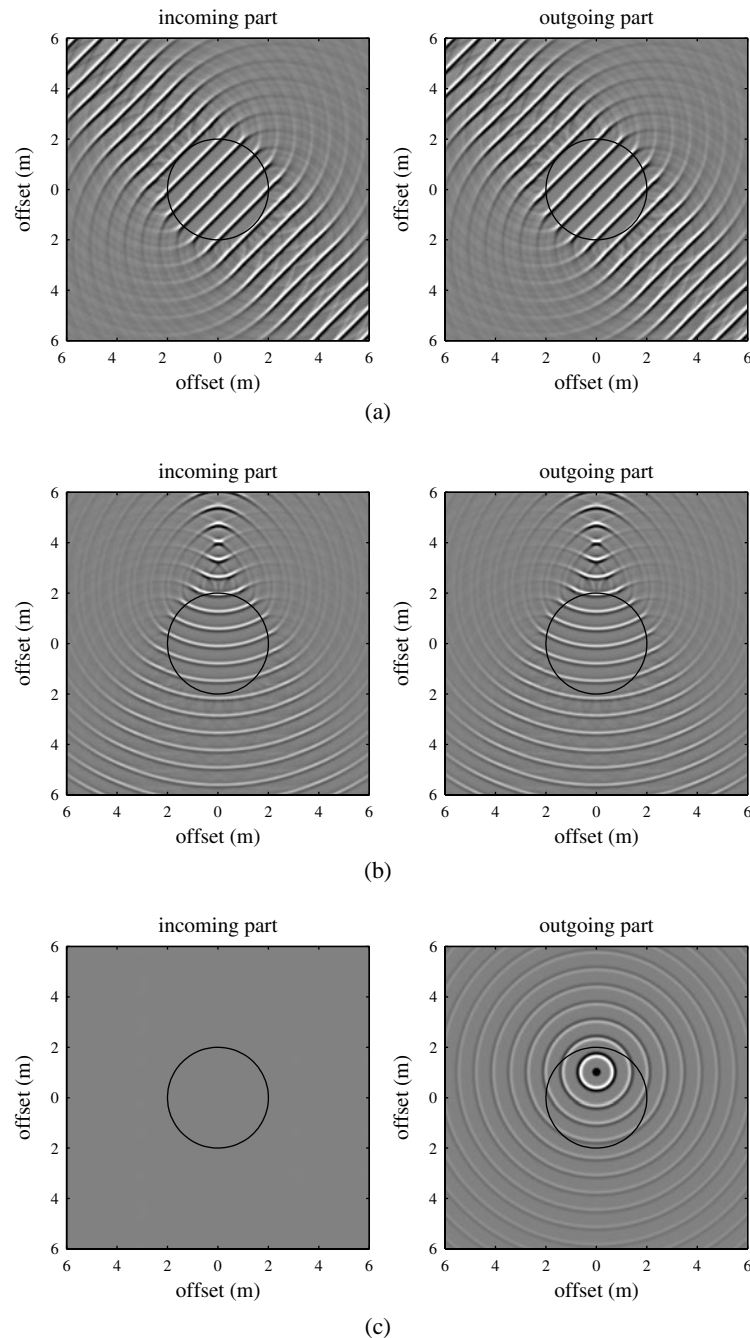
Fig. 10. Incoming and outgoing plane-wave reconstruction. (a) Plane wave. (b) Point source outside circle. (c) Point source inside circle.

7 CONCLUSIONS

Three types of recording arrays for auralization purposes have been investigated.

For linear arrays both pressure and normal velocity can be recorded to eliminate front–back crosstalk. However, due to a limited resolution of the linear array in endfire configurations, the reconstruction area of such an array is very limited. Linear arrays are therefore not suitable for state-of-the-art auralization using WFS.

The linear array can be expanded to a cross array to enlarge the reconstruction area. The reconstruction is still not perfect. Diffractions from the endpoints of the arrays are still present, and the amplitude of the reconstructed sound field is not perfect either.

The circular array performs much better. It has a homogeneous resolution and a circular reconstruction area in which no artifacts are present. The circular recording can easily be converted into incoming and outgoing cylindrical harmonics (high-order ambisonics), which in turn can easily be converted into a plane-wave decomposition. The latter two representations are equivalent. This makes each representation a very useful format for auralization and spatial sound reproduction purposes.

In this paper the circular microphone array is used for auralization purposes only, but the same theory and techniques can be applied for making live high-order ambisonic (B-format) recordings.

If one deals with a circular array recording of an impulse response in a three-dimensional hall, the three-dimensional $1/r$ amplitude decays of the recording can be converted to two dimensions, extrapolated to the proper reproduction positions in two-dimensional space using the methods described in this paper, and scaled back to three dimensions afterward. A circular array, however, is not capable of properly reconstructing sound sources at elevated angles. For that purpose a surface of microphones is required instead of a line array.

8 REFERENCES

[1] G. Naylor, "Computer Modelling and Auralisation of Sound Fields in Room," *Appl. Acoust.*, vol. 38, (1993).

[2] A. J. Berkhout, D. de Vries, and P. Vogel, "Acoustic Control by Wave Field Synthesis," *J. Acoust. Soc. Am.*, vol. 93, pp. 2764–2778 (1993).

[3] D. de Vries and J. Baan, "Auralization of Sound Fields by Wave-Field Synthesis," presented at the 106th Convention of the Audio Engineering Society, *J. Audio Eng. Soc. (Abstracts)*, vol. 47, p. 527 (1999 June), preprint 4927.

[4] A. J. Berkhout, D. de Vries, and J. J. Sonke, "Array Technology for Acoustic Wave Field Analysis in Enclosures," *J. Acoust. Soc. Am.*, vol. 102, pp. 2757–2770 (1996).

[5] A. J. Berkhout, *Applied Seismic Wave Theory*, (Elsevier, Amsterdam, The Netherlands, 1987).

[6] R. Nicol and M. Emerit "3D-Sound Reproduction over an Extensive Listening Area: A Hybrid Method Derived from Holophony and Ambisonic," in *Proc. AES 16th Int. Conf.*, pp. 436–453 (1999).

[7] J. S. Bamford, "An Analysis of Ambisonic Sound Systems of First and Second Order," Ph.D. thesis, University of Waterloo, Waterloo, Ont., Canada (1995).

[8] M. A. Poletti, "A Unified Theory of Horizontal Holographic Sound Systems," *J. Audio Eng. Soc.*, vol. 48, pp. 1155–1182 (2000 Dec.).

[9] D. T. Blackstock, *Fundamentals of Physical Acoustics* (Wiley-Interscience, New York, 2000).

[10] K. Farrar, "Soundfield Microphone," *Wireless World*, pp. 48–50 (1979 Oct.).

[11] M. A. Gerzon, "General Metatheory of Auditory Localisation," presented at the 92nd Convention of the Audio Engineering Society, *J. Audio Eng. Soc. (Abstracts)*, vol. 40, p. 447 (1992 May), preprint 3306.

[12] M. Abramowitz and I. A. Stegun, *Handbook of Mathematic Functions* (Dover, New York, 1965).

APPENDIX 1
KIRCHHOFF–HELMHOLTZ-BASED PLANE-WAVE DECOMPOSITION

In this appendix a general formula for the plane-wave decomposition is derived in terms of the Kirchhoff–Helmholtz extrapolation of a sound field. Suppose $p^{(1)}(r, \theta, \omega)$ and $p^{(2)}(r, \theta, \omega)$ are the inverse and forward extrapolated sound fields from a given array configuration to a large circle with radius r around the origin o, using the Kirchhoff–Helmholtz or Rayleigh integrals. θ is the azimuth angle on the circle (see Fig. 4). If these inverse and forward extrapolated sound fields are forward and inversely extrapolated. respectively, to the center of the circle o using the Kirchhoff–Helmholtz integrals, they become

$$p^{(1)}(o, \omega) = \frac{-jk}{4} \int_0^{2\pi} p^{(1)}(r, \theta, \omega) \, H_1^{(2)}(kr) r \, d\theta$$

$$+ \frac{-jk}{4} \int_0^{2\pi} j\rho c v_n^{(1)}(r, \theta, \omega) \, H_0^{(2)}(kr) r \, d\theta$$

$$(30)$$

$$p^{(2)}(o, \omega) = \frac{-jk}{4} \int_0^{2\pi} p^{(2)}(r, \theta, \omega) H_1^{(1)}(kr) r \, d\theta$$

$$+ \frac{-jk}{4} \int_0^{2\pi} j\rho c v_n^{(2)}(r, \theta, \omega) H_0^{(1)}(kr) r \, d\theta.$$

If we assume $kr \gg 1$, the following far-field approximations are valid:

$$v_n \approx \frac{1}{\rho c} \, p$$

$$H_n^{(1)}(kr) \approx (-j)^n \frac{1 - j}{\sqrt{\pi}} \frac{e^{jkr}}{\sqrt{kr}}$$

$$(31)$$

$$H_n^{(2)}(kr) \approx j^n \frac{1 + j}{\sqrt{\pi}} \frac{e^{-jkr}}{\sqrt{kr}}$$

and the integrals can be written as

$$p^{(1)}(\boldsymbol{o},\omega) = \frac{1+j}{\sqrt{4\pi}} \int_0^{2\pi} \sqrt{kr}\; p^{(1)}(r,\theta,\omega)\; e^{-jkr}\, d\theta$$

$$p^{(2)}(\boldsymbol{o},\omega) = \frac{1-j}{\sqrt{4\pi}} \int_0^{2\pi} \sqrt{kr}\; p^{(2)}(r,\theta,\omega)\; e^{jkr}\, d\theta \;. \tag{32}$$

These equations write the pressure at the center of the circle as an integral of contributions from the points on the circle. If the circle becomes larger, these contributions increasingly approximate plane-wave contributions. Therefore the plane-wave decompositions $s^{(1)}$ and $s^{(2)}$ are equal to the $r \to \infty$ limit of these contributions,

$$s^{(1)}(\theta,\omega) = \frac{1+j}{\sqrt{4\pi}} \lim_{r\to\infty} \sqrt{kr}\; p^{(1)}(r,\theta,\omega)\; e^{-jkr}$$

$$s^{(2)}(\theta,\omega) = \frac{1-j}{\sqrt{4\pi}} \lim_{r\to\infty} \sqrt{kr}\; p^{(2)}(r,\theta,\omega)\; e^{jkr} \;. \tag{33}$$

APPENDIX 2
DECOMPOSITION OF CIRCULAR RECORDINGS INTO CYLINDRICAL HARMONICS

In two dimensions the sound fields of these and higher order cylindrical harmonics are given by

$$\mathscr{P}^{(1)}_{k_\theta}(r,\theta,\omega) = H^{(1)}_{k_\theta}(kr)\; e^{jk_\theta\theta}$$

$$\mathscr{P}^{(2)}_{k_\theta}(r,\theta,\omega) = H^{(2)}_{k_\theta}(kr)\; e^{jk_\theta\theta} \tag{34}$$

representing the pressure fields of the incoming and outgoing cylindrical harmonics, respectively. In order to calculate the decomposition of recorded pressure and normal particle velocity in terms of cylindrical harmonics, first the radial velocity component of these cylindrical harmonics is calculated using Newton's second law,

$$-\nabla p = j\omega\rho v \;. \tag{35}$$

If this equation is transformed into cylindrical coordinates and only the inwardly directed radial component of the velocity is considered, it becomes

$$\frac{\partial p}{\partial r} = j\omega\rho v_n \;. \tag{36}$$

Using this together with the formula for the derivative of the Hankel functions [12],

$$H'^{(1)}_n = \frac{1}{2} H^{(1)}_{n-1} - \frac{1}{2} H^{(1)}_{n+1}$$

$$H'^{(2)}_n = \frac{1}{2} H^{(2)}_{n-1} - \frac{1}{2} H^{(2)}_{n+1} \tag{37}$$

the radial velocity components of the cylindrical harmon-

ics can be calculated,

$$j\rho c\,\mathscr{V}^{(1)}_{k_\theta}(r,\theta,\omega) = H'^{(1)}_{k_\theta}(kr)\; e^{jk_\theta\theta}$$

$$= \frac{1}{2}\left[H^{(1)}_{k_\theta-1}(kr) - H^{(1)}_{k_\theta+1}(kr)\right] e^{jk_\theta\theta} \tag{38}$$

$$j\rho c\,\mathscr{V}^{(2)}_{k_\theta}(r,\theta,\omega) = H'^{(2)}_{k_\theta}(kr)\; e^{jk_\theta\theta}$$

$$= \frac{1}{2}\left[H^{(2)}_{k_\theta-1}(kr) - H^{(2)}_{k_\theta+1}(kr)\right] e^{jk_\theta\theta} \;. \tag{38}$$

To decompose the circular recording into cylindrical harmonics, $\mathscr{M}^{(1)}(k_\theta, \omega)$ and $\mathscr{M}^{(2)}(k_\theta, \omega)$ have to be chosen such that

$$p(\theta,\omega) = \sum_{k_\theta}\mathscr{M}^{(1)}(k_\theta,\omega)\,\mathscr{P}^{(1)}_{k_\theta}(R,\theta,\omega)$$

$$+ \sum_{k_\theta}\mathscr{M}^{(2)}(k_\theta,\omega)\,\mathscr{P}^{(2)}_{k_\theta}(R,\theta,\omega)$$

$$v_n(\theta,\omega) = \sum_{k_\theta}\mathscr{M}^{(1)}(k_\theta,\omega)\,\mathscr{V}^{(1)}_{k_\theta}(R,\theta,\omega) \tag{39}$$

$$+ \sum_{k_\theta}\mathscr{M}^{(2)}(k_\theta,\omega)\,\mathscr{V}^{(2)}_{k_\theta}(R,\theta,\omega) \;.$$

To solve these equations it is convenient to take the Fourier transforms of p and v with respect to θ,

$$P(k_\theta,\omega) = \frac{1}{2\pi}\int_0^{2\pi} p(\theta,\omega)\; e^{-jk_\theta\theta}\, d\theta$$

$$V_n(k_\theta,\omega) = \frac{1}{2\pi}\int_0^{2\pi} v_n(\theta,\omega)\; e^{-jk_\theta\theta}\, d\theta \;. \tag{40}$$

The Fourier series can now be written as

$$p(\theta,\omega) = \sum_{k_\theta} P(k_\theta,\omega)\; e^{jk_\theta\theta}$$

$$v_n(\theta,\omega) = \sum_{k_\theta} V_n(k_\theta,\omega)\; e^{jk_\theta\theta} \;. \tag{41}$$

If the left-hand terms of Eqs. (30) are replaced by these Fourier series, they become

$$P(k_\theta,\omega) = \mathscr{M}^{(1)}(k_\theta,\omega)\, H^{(1)}_{k_\theta}(kR)$$

$$+ \mathscr{M}^{(2)}(k_\theta,\omega)\, H^{(2)}_{k_\theta}(kR)$$

$$j\rho cV_n(k_\theta,\omega) = \mathscr{M}^{(1)}(k_\theta,\omega)\, H'^{(1)}_{k_\theta}(kR) \tag{42}$$

$$+ \mathscr{M}^{(2)}(k_\theta,\omega)\, H'^{(2)}_{k_\theta}(kR) \;.$$

This set can now be solved, term by term, for $\mathscr{M}^{(1)}$ and

$\mathscr{M}^{(2)}$ in terms $P(k_\theta, \omega)$, and $V_n(k_\theta, \omega)$,

$$\mathscr{M}^{(1)}(k_\theta, \omega)$$
$$= \frac{H'^{(2)}_{k_\theta}(kR)\, P(k_\theta, \omega) - H^{(2)}_{k_\theta}(kR)\, j\rho c V_n(k_\theta, \omega)}{H^{(1)}_{k_\theta}(kR)\, H'^{(2)}_{k_\theta}(kR) - H^{(2)}_{k_\theta}(kR)\, H'^{(1)}_{k_\theta}(kR)}$$

(43)

$$\mathscr{M}^{(2)}(k_\theta, \omega)$$
$$= \frac{H'^{(1)}_{k_\theta}(kR)\, P(k_\theta, \omega) - H^{(1)}_{k_\theta}(kR)\, j\rho c V_n(k_\theta, \omega)}{H^{(2)}_{k_\theta}(kR)\, H'^{(1)}_{k_\theta}(kR) - H^{(1)}_{k_\theta}(kR)\, H'^{(2)}_{k_\theta}(kR)}.$$

$\mathscr{M}^{(1)}$ and $\mathscr{M}^{(2)}$ are the expansion coefficients of the sound field in terms of cylindrical harmonics [see Eqs. (39)].

THE AUTHORS

E. Hulsebos

D. de Vries

E. Bourdillat

Edo Maria Hulsebos was born August 28, 1974, in Deventer, Gelderland, The Netherlands. He received his primary and secondary education in Twello and Deventer. In 1992 he participated in the International Physics Olympiad in Helsinki, Finland. In that same year he started physics studies at Utrecht University. He received an M.Sc. degree in 1999 for research on spaciousness in room acoustics done in the laboratory of Acoustical Imaging and Sound Control at the Delft University of Technology. He is currently working on his Ph.D. thesis, "Recording and Reproduction of Audio and Room Acoustics Using Array Technology," in the same laboratory. He has presented a number of papers on this topic at recent AES conventions.

●

Diemer de Vries was born January 3, 1945, in Weststellingwerf, Friesland, The Netherlands. He received his primary and secondary education at schools in Arnhem, Heemstede, and Haarlem, The Netherlands. He received an applied physics degree, an M.Sc. degree for a thesis on architectural acoustics, and a Ph.D. degree for a thesis on seismic signal processing from the Delft University of Technology in 1963, 1971, and 1984, respectively.

After graduating in 1971, he joined the staff of the Laboratory of Acoustics (now Seismics and Acoustics) at Delft University. During his career as a university researcher, he worked on several projects in room acoustics, building acoustics, and seismic signal processing. He now coordinates, as an associate professor, the research on wave-field analysis and synthesis in room acoustics. During the summer semester of 2001, he fulfilled the Edgard Varese guest professorship at the TU Berlin.

As a specific form of applied acoustics, Dr. de Vries plays the double bass in The Hague Baroque Company and several chamber music and, on request, jazz ensembles.

He received a Certificate of Appreciation in 1995 from the AES Netherlands Section and an AES Fellowship Award in 1999 for his contributions to the implementation of wave-field synthesis in audio technology.

●

Emmanuelle S. Bourdillat was born in Suresnes, France, in 1975. She studied applied physics at the Universite de Paris VII, where she received a Licence and a Maitrise. In 2000 she joined the Delft acoustics group as a student to work on the perceptual properties of sound fields recorded with microphone arrays and auralized by means of wave-field synthesis from which she received an M.Sc. degree in 2001.

Currently Ms. Bourdillat works as an acoustic consultant for Hoover & Keith in Houston, Texas, USA.